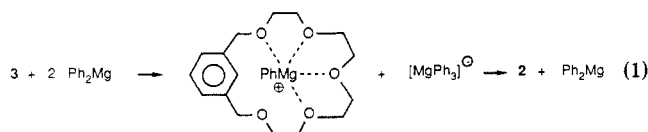


Figure 1. PLUTON drawing of **2**. Selected bond distances (Å) and angles (deg): Mg–C(17), 2.189 (5); Mg–C(23), 2.190 (5); Mg–O(2), 2.204 (3); Mg–O(3), 2.222 (4); Mg–O(1) 2.516 (4); Mg–O(4), 2.520 (4); C(17)–Mg–C(23), 163.8 (2); C(17)–Mg–O(2), 96.9 (2); C(17)–Mg–O(3), 96.9 (2); C(23)–Mg–O(2), 96.1 (2); C(23)–Mg–O(3), 95.9 (2); O(2)–Mg–O(3), 74.6 (1).

X-ray structure of **2** (Figure 1) is its rotaxane character: the diphenylmagnesium is almost linear and rod-shaped with bulky end groups and sticks through the cavity of the coordinating crown ether ring of ligand **3**.

The magnesium shows an unusual type of hexacoordination: besides to the two apical carbons in the nearly sp -hybridized,⁸ covalent Ph–Mg–Ph unit (angle C(17)–Mg–C(23) = 163.8 (2)°; dihedral angle between the two phenyl rings: 66.2 (2)° magnesium is rather tightly bound to O(2) and O(3), and less so to O(1) and O(4); O(1)–O(4) and magnesium form, within 0.037 (7) Å, a quasi-equatorial plane, and O(5) is clearly not participating in the coordination ($d(\text{Mg}–\text{O}(5)) = 4.038$ (3) Å). The aromatic ring of the ligand makes an oblique angle with the equatorial plane. As in the $[\text{AlMe}_2\cdot 18\text{-crown-6}]^+$ cation,² the folding of the C–M–C unit is directed away from the coordinating oxygens.

Another interesting feature of **2** concerns the presumable mode of its formation. The cavity of the ligand **3** is too small to permit direct penetration of a phenyl ring of diphenylmagnesium. Complex formation must therefore occur by dissociation of a phenyl anion, complexation of the PhMg^+ cation, and recombination with the phenyl anion from the other side. In view of known analogous dissociation processes,^{1,2} the phenyl anion is probably incorporated into an ate complex, and the course of events may be depicted as in eq 1. Dissolved in toluene- d_8 , **2** gives rise to



two clearly distinguishable complexes (**4a**: **4b** = 3:1), while uncomplexed diphenylmagnesium and **3** (cf. ref 2d) are absent.⁹ We assume that **4a** has the rotaxane structure of **2**, because the resonance of H(2) ($\delta = 9.02$ ppm) is strongly shifted downfield relative to the corresponding signal of **3** ($\delta = 8.16$ ppm) or of **4b** ($\delta = 8.24$ ppm), presumably due to steric congestion.¹⁰ The close

similarity between the resonances of **3** and **4b** suggests that in **4b** diphenylmagnesium is externally coordinated to some of the oxygens of **3**. It is remarkable that the two complexes differ so little in stability; in THF- d_8 solution, **2** is completely dissociated into its components.⁹

Acknowledgment. We thank A.J.M. Duisenberg for collecting the X-ray data. The investigations were supported in part (P.R.M., W.J.J.S., and A.L.S.) by the Netherlands Foundation for Chemical Research (SON) with financial aid from the Netherlands Organization for Advancement of Pure Research (ZWO); we also thank ZWO for a visiting scholarship (T.N.).

Registry No. **2**, 114691-81-5; **3**, 53914-83-3; Ph_2Mg , 555-54-4.

Supplementary Material Available: Tables of fractional atomic coordinates, anisotropic thermal parameters, all bond distances and angles and Figure 2 (ORTEP drawing of **2**) (6 pages); listings of observed and calculated structure factors of **2** (22 pages). Ordering information is given on any current masthead page.

(9) ^1H NMR of a solution of pure **2** in toluene- d_8 (250 MHz, $\text{C}_6\text{D}_6/\text{CHD}_2$ (δ (^1H) 2.32 ppm) as internal standard): **4a** δ 2.89–2.93 and 2.96–3.00 (m, A_2B_2 , 8 H, C_2H_4), 3.03–3.07 and 3.18–3.27 (m, A_2B_2 , 8 H, C_2H_4), 4.44 (s, 4 H, xylyl- CH_2), 7.15 (dd, $^3J = 7$ Hz, $^4J = 1$ Hz, 2 H, xylyl-H(4,6)), 7.47 (tt, $^3J = 7$ Hz, $^2J = 2$ Hz, 2 H, phenyl-H(4)), 7.59 (dd, $^3J = 8$ Hz, $^2J = 7$ Hz, 4 H, phenyl-H(3,5)), 8.09 (dd, $^3J = 8$ Hz, $^4J = 2$ Hz, 4 H, phenyl-H(2,6)), 9.02 (m, 1 H, xylyl-H(2)). **4b** δ 3.11–3.15 (m, A_2B_2 , 8 H, C_2H_4), 3.18–3.22 and 3.34–3.38 (m, A_2B_2 , 8 H, C_2H_4), 4.54 (s, 4 H, xylyl- CH_2), 6.96 (dd, $^3J = 7$ Hz, $^4J = 1$ Hz, 2 H, xylyl-H(4,6)), 7.47 (tt, 2 H, phenyl-H(4), coinciding with those of **4a**), 7.66 (dd, $^3J = 8$ Hz, $^2J = 7$ Hz, 4 H, phenyl-H(3,5)), 8.44 (dd, $^3J = 8$ Hz, $^4J = 2$ Hz, 4 H, phenyl-H(2,6)), 8.24 (m, 1 H, xylyl-H(2)). The resonances of the protons xylyl-H(5) of **4a** and **4b** could not be assigned; probably, they coincide with other signals of **4a**, **4b** or toluene- d_8 (δ 7.2, 7.25, 7.33). The relative amounts of **4a** and **4b** and the position of phenyl-H(4) of **4b** were determined from the integral ratios. ^1H NMR of a solution of pure **2** in THF- d_8 (250 MHz, β -H of THF- d_7 (δ 1.75 ppm) as internal standard): diphenylmagnesium δ 6.90 (tt, $^3J = 7.2$ Hz, $^4J = 1.5$ Hz, 2 H, H(4)), 6.99 (dd, $^3J = 7.3$ Hz, $^2J = 7.2$ Hz, 4 H, H(3,5)), 7.72 (dd, $^3J = 7.3$ Hz, $^4J = 1.5$ Hz, H(2,6)). **3**: δ 3.57–3.66 (m, A_2B_2 , 16 H, C_2H_4), 4.57 (s, 4 H, xylyl- CH_2), 7.09 (dd, $^3J = 7$ Hz, $^4J = \text{ca. } 1$ Hz, 2 H, xylyl-H(4,6)), 7.21 (t, $^3J = 7$ Hz, 1 H, xylyl-H(5)), 7.70 (m, 1 H, xylyl-H(2)).

(10) (a) Jackman, L. M.; Sternhell, S. *Applications of Nuclear Magnetic Resonance Spectroscopy in Organic Chemistry*, 2nd ed.; Pergamon Press: Oxford, 1969; p 71. (b) Sato, T.; Takemura, T.; Kainosho, M. *J. Chem. Soc., Chem. Commun.* 1974, 97. (c) Van Straten, J. W.; De Wolf, W. H.; Bickelhaupt, F. *Tetrahedron Lett.* 1977, 4667.

Bis(2,3,4,6,7- η^5 -bicyclo[3.2.2]nona-2,6,8-trien-4-yl)iron, a Ferrocene Analogue with Separated Allyl and Olefin Systems

Janet Blümel, Frank H. Köhler,* and Gerhard Müller

Anorganisch-chemisches Institut
Technische Universität München
D-8046 Garching, Federal Republic of Germany

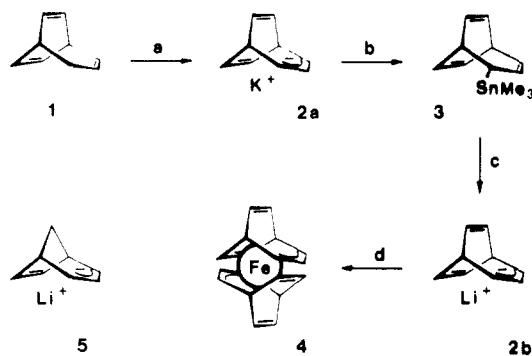
Received March 2, 1988

It is a long-standing question in organic chemistry whether carbanions like bicyclo[3.2.2]nona-2,6,8-trien-4-yl (BCNT) anion **2** or the congener **5** (cf. Scheme I) experience some extra stabilization by homoaromatic interaction of the allyl and the olefin part(s) of the molecule. It dates back to early studies¹ and even the most recent calculations² and experiments³ find arguments

(1) (a) Brown, J. M. *Chem. Commun.* 1967, 638. (b) Winstein, S.; Ogliaruso, M.; Sakai, M.; Nicholson, J. M. *J. Am. Chem. Soc.* 1967, 89, 3656. (c) Grutzner, J. B.; Winstein, S. *Ibid.* 1972, 94, 2200.

(2) (a) Schleyer, P. v. R.; Kaufmann, E.; Kos, A. J.; Mayr, H.; Chandrasekhar, J. *J. Chem. Soc., Chem. Commun.* 1986, 1583. (b) Lindh, R.; Roos, B. O.; Jonsäll, G.; Ahlberg, P. *J. Am. Chem. Soc.* 1986, 108, 6554. (c) Brown, J. M.; Elliot, R. J.; Richards, W. G. *J. Chem. Soc., Perkin Trans. 2* 1982, 485. (d) Grutzner, J. B.; Jørgensen, W. L. *J. Am. Chem. Soc.* 1981, 103, 1372. (e) Kaufmann, E.; Mayr, H.; Chandrasekhar, J.; Schleyer, P. v. R. *Ibid.* 1981, 103, 1375.

(8) The normal hybridization of magnesium in monomeric uncoordinated R_2Mg seems to be sp ; cf. bis(neopentyl)magnesium: Ashby, E. C.; Fernholt, L.; Haaland, A.; Seip, R.; Scott Smith, R. *Acta Chem. Scand.* 1980, A34, 213.

Scheme 1^a

^a (a) *n*-BuLi/*t*-BuOK, pentane, $-78\text{ }^{\circ}\text{C}$. (b) Me_3SnCl . (c) MeLi, THF, $-78\text{ }^{\circ}\text{C}$. (d) $\text{FeCl}_2 \cdot 1.5\text{THF}$.

pro and contra homoaromaticity although the counterion is now accepted to play an important role in the stabilization of **5**. From a more practical and organometallic point of view we have simplified the problem by asking the following question: How similar are the cyclopentadienyl anion (Cp^-) and **2** or **5**? Here we report on a new short access to the anion **2** and on the prototype **4** of a metallocene-like derivative.

2a has been prepared from cycloheptatriene in nine steps.^{1b} When **1**,⁵ obtained in three steps from cycloheptatriene,⁴ is treated with *n*-BuLi/*t*-BuOK **2a** is produced in more than 77% yield as shown by stannylation to **3**.⁵ Transmetalation leads to **2b** in quantitative⁶ yield. Its ¹³C data differ somewhat from those in ref 3a and 7 due to experimental details which we have found to seriously affect the NMR spectra of the analogous anion **5**.^{3d} Addition of iron(II) chloride to **2b** in THF provides a brown solution, and after replacing the ether by pentane slow evaporation and cooling to $-30\text{ }^{\circ}\text{C}$ gives orange crystals of **4**.⁸

The molecular geometry of **4** in the solid state is presented in Figure 1.⁹ Two BCNT ligands are bound to iron in a η^5 -fashion. Complex **4** is strictly centrosymmetric, implying opposite orientation of the two BCNT ligands with respect to each other. One of the two BCNT double bonds (C6–C7 1.365 (3) Å) is bound to iron; it is significantly longer than the other one (C8–C9 1.320 (3) Å). A typical metal–allyl bond forms between C2, C3, C4,

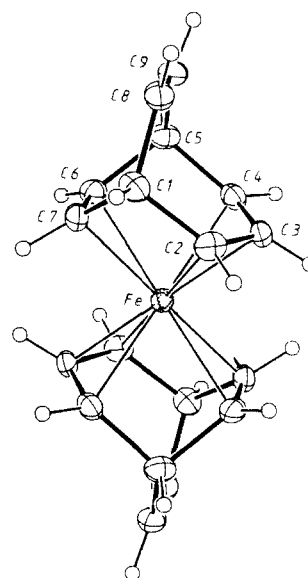


Figure 1. ORTEP representation of the molecular geometry of **4** (displacement ellipsoids at the 50% probability level; H-atoms with arbitrary radii). Selected bond lengths (Å): C2–C3 1.415 (3), C3–C4 1.404 (3), C6–C7 1.365 (3), C8–C9 1.320 (3), Fe–C2 2.155 (2), Fe–C3 2.054 (2), Fe–C4 2.154 (2), Fe–C6 2.163 (2), Fe–C7 2.165 (2). Interplanar angles (deg): A/B 103.7, A/C 117.5, B/C 138.7, with A = C1, C2, C4, C5, B = C1, C5, C6, C7, C = C1, C5, C8, C9.

and iron with Fe–C3 being ca. 0.1 Å shorter than the other iron–carbon bonds. A “separate” allyl system is further suggested by the fact that its plane is inclined by 22.2° relative to the neighboring plane A (cf. Figure 1). Thus C3 is bent away from Fe similarly as is C3 from Li in **5**·TMEDA.^{3d} The interplanar angles A/B, A/C, and B/C reorganize on bonding to the metal so that A/B (103.7°) becomes rather small and hence the allyl and one olefinic part (C6/7) of BCNT move closer. This is manifested in C2...C7 and C4...C6 distances of 2.33 Å¹⁰ and should favor homoconjugation.^{2c} The least-squares planes through C2, C3, C4, C6, C7 and their symmetry equivalent counterparts resemble the Cps of ferrocene, but in **4** these planes are only 2.99 Å apart while 3.30 Å has been reported¹¹ for ferrocene. There is also a bending of the hydrogen atoms (refined) out of their adjacent C-atom planes even for H8/9 ($5.6/4.8^{\circ}$ toward C3) although C8/9 are not involved in metal bonding. Again the allyl and olefin part behave differently: H2/3/4 are bent toward iron ($8.0/14.0/0.5^{\circ}$) while H6/7 are bent away ($10.1/8.4^{\circ}$). Apparently, the geometry of **4** is mainly determined by the metal–ligand bonding; whether this leads to an increased homoaromaticity in the ligand remains unclear.

4 is thermally less stable than ferrocene and decomposes above $50\text{ }^{\circ}\text{C}$. In cyclic voltammetry¹² **4** undergoes a reversible oxidation; as compared to internal ferrocene it occurs 530 mV more cathodic. A similar potential shift $E_{1/2}$ has been observed for decamethylferrocene,^{13a} and it is known that methylation of ferrocene and interrupting the conjugation in the ligand lead to parallel trends for $E_{1/2}$.^{13b}

Several enlightening changes of the NMR data⁸ emerge when we pass from **1** to **4**. The decrease of the number of signals implies C_s symmetry for the ligand but not necessarily C_{2h} for **4** in solution. The double bonds become inequivalent with dramatic complexation shifts ($\Delta\delta(\text{C6/7})$ ca. -97 , $\Delta\delta(\text{H6/7})$ ca. -3) and the appearance

(3) (a) Jonsäll, G.; Ahlberg, P. *J. Chem. Soc., Perkin Trans. 2* **1987**, 461. (b) Christl, M.; Brückner, D. *Chem. Ber.* **1986**, *119*, 2025. (c) Lee, R. E.; Squires, R. R. *J. Am. Chem. Soc.* **1986**, *108*, 5078. (d) Hertkorn, N.; Köhler, F. H.; Müller, G.; Reber, G. *Angew. Chem.* **1986**, *98*, 462; *Angew. Chem., Int. Ed. Engl.* **1986**, *25*, 468. (e) Christl, M.; Leininger, H.; Brückner, D. *J. Am. Chem. Soc.* **1983**, *105*, 4848. (f) Köhler, F. H.; Hertkorn, N. *Chem. Ber.* **1983**, *116*, 3274. (g) Washburn, W. N. *J. Org. Chem.* **1983**, *48*, 4287. (4) Tsuji, T.; Ishitobi, H.; Tanida, H. *Bull. Chem. Soc. Jpn.* **1971**, *44*, 2447.

(5) Detailed NMR data (1: $\delta(^{13}\text{C})$, $\delta(^1\text{H})$, $^1J(^{13}\text{C}-^1\text{H})$, $^nJ(^1\text{H}-^1\text{H})$; 3: $\delta(^{119}\text{Sn})$, $\delta(^{13}\text{C})$, $^nJ(^{119}\text{Sn}-^{13}\text{C})$; 2b: $\delta(^{13}\text{C})$) are given in the Supplementary Material.

(6) No **3** can be detected in the reaction mixture by ¹³C NMR.

(7) Goldstein, M. J.; Tomoda, S.; Wittacker, G. *J. Am. Chem. Soc.* **1974**, *96*, 3676.

(8) ¹H NMR (270 MHz, C_6D_6 , $30\text{ }^{\circ}\text{C}$): δ 2.67, 2.94, 3.17, 3.37, 5.75 (H1/5, 2/4, 3, 6/7, 8/9); $^3J(\text{Hx}-\text{Hy})$ in Hz = 7.5 (1–2), 5.3 (1–7), 4.6 (1–8), 7.0 (2–3), $^4J(\text{H6}-\text{H9})$ = 3.1 Hz. ¹³C NMR (67.8 MHz, C_6D_6 , $30\text{ }^{\circ}\text{C}$): $\delta/1J(\text{CH})$ in Hz 31.55/139.7, 30.71/165.7, 83.93/161.9, 37.19/169.1, 132.76/160.5 (C1/5, 2/4, 3, 6/7, 8/9); assignments confirmed by selective ¹H/¹³C NMR experiments.

(9) Crystal structure data for **4**: Syntax-P2₁ diffractometer, Mo K α radiation, λ = 0.71069 Å, graphite monochromator, T = $-35\text{ }^{\circ}\text{C}$. $\text{C}_{18}\text{H}_{18}\text{Fe}$, M_r = 290.19, monoclinic, space group $P2_1/n$ (No. 14), a = 6.320 (1) Å, b = 10.650 (1) Å, c = 9.163 (1) Å, β = $95.89(1)^{\circ}$, V = 613.5 Å³, d_{calc} = 1.571 g/cm³ for Z = 2, $\mu(\text{Mo K}\alpha)$ = 12.1 cm⁻¹, $F(000)$ = 304. 2112 reflections were measured up to $(\sin \theta/\lambda)_{\text{max}}$ = 0.638 Å⁻¹ ($+h, \pm k, \pm l$, ω scan, $\Delta\omega$ = 0.9°). The data were corrected for Lp effects and empirically for absorption (relative transmission: 0.83–1.00). Merging of equivalent data yielded 1327 unique structure factors (R_{int} = 0.021), 1222 of which had $F_0 \geq 4.0\sigma(F_0)$. The structure was solved by Patterson methods. All hydrogen atoms were located in difference syntheses and refined isotropically. All other atoms were treated anisotropically. R (R_w) = 0.034 (0.043), $w = 1/\sigma^2(F_0)$ for 124 refined parameters and all unique reflections (SHELX-76); $\Delta\rho_{\text{max}}$ (max/min) = 0.39/0.40 e/Å³. See note at the end of the paper for Supplementary Material Available.

(10) Cf. 2.46 Å for the corresponding distance in barrelene. Yamamoto, S.; Nakata, M.; Fukujama, T.; Kuchitsu, K.; Hasselmann, D.; Ermer, O. *J. Phys. Chem.* **1982**, *86*, 529.

(11) Seiler, P.; Dunitz, J. D. *Acta Crystallogr., Sect. B* **1979**, *36*, 2020 and literature cited therein.

(12) $\text{THF}/[n\text{-Bu}_4\text{N}]\text{PF}_6$, 4.3×10^{-4} mol·L⁻¹ **4** and 1.0×10^{-3} mol·L⁻¹ Cp_2Fe , 50 mV s⁻¹, $25\text{ }^{\circ}\text{C}$; $I_{\text{pa}}/I_{\text{pc}}$ = 0.98 without Cp_2Fe .

(13) (a) Robbins, J. L.; Edelstein, N.; Spencer, B.; Smart, J. C. *J. Am. Chem. Soc.* **1982**, *104*, 1882. (b) Eischenbroich, Ch.; Bilger, E.; Ernst, R. D.; Wilson, D. R.; Kralik, M. S. *Organometallics* **1985**, *4*, 2068.

of a coupling between the olefinic protons. $^1J(C6/7-H6/7)$ increases on bonding to iron whereas it decreases on bonding to lithium in **2b**,⁵ which means that charge transfer to and rehybridization at C6/7 do not dominate the coupling.

The isolation of **4** shows that even if the π -system of Cp anions is broken down into olefinic and allylic systems bonding to transition metals is still possible. "Opening" Cp ligands once as realized in metal-pentadienyl chemistry¹⁴ is not the ultimate perturbation that π -complexes tolerate.

Acknowledgment is made to the Fonds der Chemischen Industrie for a scholarship (J.B.) and support of this research.

Supplementary Material Available: NMR data⁵ of **1**, **2a**, and **3** and complete tables of atomic coordinates and displacement parameters for **4** (7 pages); listing of observed and calculated structure factors for **4** (8 pages). Ordering information is given on any current masthead page.

(14) Recent contributions: (a) Kralik, M. S.; Rheingold, A. L.; Ernst, R. D. *Organometallics* **1988**, 6, 2612. (b) Bleeke, J. R.; Rauscher, D. J.; Moore, D. A. *Ibid.* **1988**, 6, 2614.

Modification of Photochemical Reactivity by Zeolites: Norrish Type I and Type II Reactions of Benzoin Derivatives

D. R. Corbin, D. F. Eaton, and V. Ramamurthy*

Central Research and Development Department[†]
E. I. du Pont de Nemours and Company
Experimental Station, Wilmington, Delaware 19898
Received January 20, 1988

Selectivity in organic phototransformations continues to be one of the main topics of current interest.¹ Of the various approaches use of constrained and ordered media has shown considerable promise.² By the utilization of the cage effect³ and conformational control we illustrate below that one can induce molecules included in zeolites to follow reaction pathways that are improbable in isotropic solvents.

The photochemical behavior of benzoin alkyl ethers (**1a**) and alkyl deoxy benzoin (**2a**) in solution are fairly well understood.^{4,5} In benzene, the former prefers the Norrish type II pathway while the latter gives the Norrish type I products in high yields (Scheme I). Photolyses of alkyl benzoin ethers and alkyl deoxy benzoin in zeolites⁶ show a dramatic difference in behavior when compared to that in benzene (Table I). Results on benzoin methyl ether and propyl deoxy benzoin in faujasite zeolite (M-X type)⁷ alone

[†] Contribution No. 4643.

(1) Ramamurthy, V. *Tetrahedron* **1986**, 42, 5753.

(2) Fox, M. A., Ed *Organic Phototransformations in Non-homogeneous Media*; American Chemical Society: Washington D.C., 1985. Ramamurthy, V.; Scheffer, J. R.; Turro, N. J., Eds. *Tetrahedron* **1987**, 43, 1197-1745. Kalyanasundaram, K. *Photochemistry in Microheterogeneous Systems*; Academic: New York, 1987.

(3) Turro, N. J.; Kraeutler, B. *Acc. Chem. Res.* **1980**, 13, 369. Cage effect in zeolites has earlier been established in the case of dibenzyl ketones: Turro, N. J. *Pure Appl. Chem.* **1986**, 58, 1219.

(4) Lewis, F. D.; Lauterbach, R. L.; Heine, H. G.; Hartmann, W.; Rudolph, H. *J. Am. Chem. Soc.* **1975**, 97, 1519. de Mayo, P.; Nakamura, A.; Tsang, P. W. K.; Wong, S. K. *J. Am. Chem. Soc.* **1982**, 104, 6824. Dasaratha Reddy, G.; Usha, G.; Ramanathan, K. V.; Ramamurthy, V. *J. Org. Chem.* **1986**, 51, 3085.

(5) Heine, H. G.; Hartmann, W.; Kory, D. R.; Magya, J. G.; Hoyle, C. E.; McVey, J. K.; Lewis, F. D. *J. Org. Chem.* **1974**, 39, 691. Lewis, F. D.; Hoyle, C. E.; Magyar, J. G.; Heine, H. G.; Hartmann, W. *J. Org. Chem.* **1975**, 40, 488. Dasaratha Reddy, G.; Ramamurthy, V. *J. Org. Chem.* **1987**, 52, 5521.

(6) Benzoin ethers and deoxy benzoin were included in zeolites by stirring known amounts of the guest and the host in trimethylpentane for 10 h. The complex was filtered and washed with ether under dry nitrogen atmosphere. Known amounts of the complex was degassed (10^{-4} Torr) and irradiated under sealed conditions. Products were extracted by stirring the irradiated complex in 10 mL of ether for 12 h. For comparison the products were also extracted by dissolving the zeolite with HCl. Material balance was ~90% in all cases. Amounts of the guest included were estimated by elemental analysis of the zeolite and by GC analysis of the reextracted material.

Scheme I

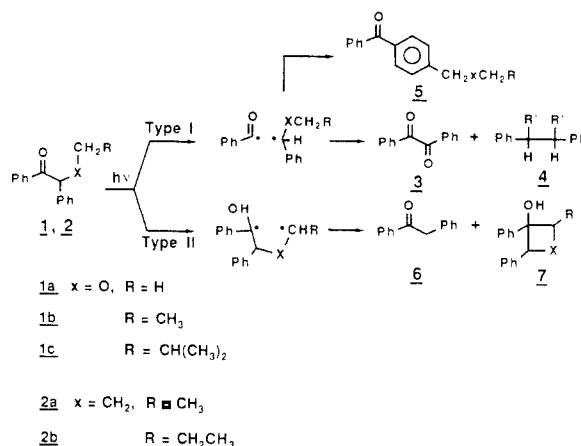


Table I. Product Distribution upon Photolysis of Benzoin Methyl Ether and Propyl Deoxy Benzoin in Zeolites

medium	percentage of products				ratio of products	
	3, 4	5	6	7	5/ 6 + 7	3 + 4 + 5/ 6 + 7
(a) Benzoin Methyl Ether						
benzene	26, 66	0.2	1.1	7	0.03	12.2
Li-X (dry)	3	76	13	8	3.6	3.6
Li-X (wet)	18	40	19	23		
Na-X (dry)	4	72	10	14	2.9	3.1
Na-X (wet)	22	47	11	20		
K-X (dry)	24	44	14	18	1.5	2.2
Rb-X (dry)	15	46	17	22	1.1	1.5
Cs-X (dry)	31	34	15	20	0.9	1.9
(b) Propyl Deoxy Benzoin						
benzene	5, 19		54	22	0	0.3
Li-X (dry)		95	4	1	18.5	
Na-X (dry)		88	5	7	7.6	
K-X (dry)		51	35	14	1.1	
Rb-X (dry)		48	31	21	0.9	
Cs-X (dry)		32	42	26	0.5	

^a Product yields (relative) were measured at ~15% conversion by gas chromatography with *cis*-stilbene as the internal standard; error limit $\pm 5\%$. ^b Wet zeolite complexes were prepared by exposing the dry complex to atmospheric moisture; zeolites made wet prior to inclusion did not include benzoin methyl ether. ^c Extraction by dissolution of the zeolite framework with HCl gave the same products (and in the same yields) as those on ether extraction. Pinacol ether and other products were stable to acid. ^d Loading in all cases was about 2% by weight as estimated by carbon analysis and re-extraction. Loading variation carried out with NaX and NaY indicated that the product distribution is independent of the loading in the range 0.5-5% by weight. ^e ZSM-5, -8, and -11 did not include benzoin methyl ether and propyl deoxy benzoin.

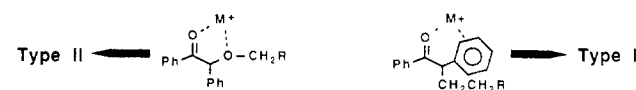


Figure 1.

are highlighted in Table I. Similar behavior was observed in M-Y zeolites. Identical behavior was found for other alkyl-substituted benzoin ethers (**1b,c**) and deoxy benzoin (**2b**).

With **1a** the amount of the type II products is considerably increased over that observed in benzene. Even more importantly, the rearrangement product, benzoylbenzyl alkyl ether (**5**), was

(7) Zeolites 13X (Na-X) and LZ-Y52 (Na-Y) were obtained from Linde. The cation of interest was exchanged into these powders by contacting the material with the appropriate nitrate solution at 90 °C. For each gram of zeolite, 10 mL of a 10% nitrate solution was used. This was repeated a number of times. The samples were then thoroughly washed with water and dried. Exchange loadings were typically between 40 and 90%. Prior to use the samples were heated in air at 1 deg/min to 500 °C and held at 500 °C for 7 h. The samples were removed at 100 °C and stored under anhydrous conditions.